MICROMECHANICAL ANALYSIS OF STRAIN RATE EFFECTS ON DAMAGE EVOLUTION IN DISCONTINUOUS FIBRE COMPOSITES

Z. Jendli[1], F. Meraghni [2], J. Fitoussi[1], and D. Baptiste[1]

[1]LM3 UMR-CNRS 8006, ENSAM Paris, 151 bd de l'Hôpital 75013 Paris, France.
[2]LMPF JE 2381, ENSAM CHÂLONS EN CHAMPAGNE, rue Saint Dominique, BP 508. 51006 CHÂLONS EN CHAMPAGNE, France.

ABSTRACT

Material overall mechanical behaviour varies significantly under rapid straining as compared to quasi-static loading. Analysing the damaged elastic behaviour of composite materials under dynamic loading requires theoretical tools and experimental approaches integrating the strain rate effects. This work is concerned with development and optimisation of an experimental methodology devoted to the micro and macroscopic characterisation of composites mechanical behaviour under high-speed loadings. The applied experimental procedure has been optimised in an attempt to isolate the inherent inertial disturbances attributed to the test system. The optimisation aims at minimizing the amplitude of measurements perturbation in order to give rise to homogeneous stress/strain fields within the tested specimen. Using a servo-hydraulic machine, monotonic and interrupted tensile tests were performed at different strain rates and coupled to scanning electronic microscope observations. The developed approach has been applied at strain rates up to 200 s^{-1} for SMC-R26 composite material.

1. INTRODUCTION

While metals have been studied extensively over a wide range of strain rates, limited information is available with regard to the effects of strain rate on composite mechanical performances. Mechanical response of fibre reinforced polymer composites under low and high-speed loading is not well understood. In fact, investigating dynamic behaviour of composites requires the development of an experimental methodology able to describe efficiently load-rate effects. Success with the high strain rate testing of polymer composites depends widely on the ability to isolate the inherent inertial disturbances attributed to the test system [1-6, 8].

The primary objective of the present work is to set up and optimise an experimental approach aimed at characterising the mechanical behaviour of composite materials subjected to rapid loadings. The experimental methodology is built upon monotonic and interrupted rapid tensile tests and were coupled to microscopic observations using scanning electronic microscopic. Tensile testes were performed at different crosshead velocities yielding to strain rates from $\dot{\varepsilon}=2.10^{-4}\ s^{-1}$(quasi-static) to $\dot{\varepsilon}=200s^{-1}$. On the one hand, this study intended to quantify the strain-rate effects on the overall behaviour in terms of elastic properties, damage and ultimate characteristics. On the other hand, it contributes to investigate local processes involving damage initiation and growth. Nevertheless, high-speed mechanical testing of polymer composites arises specific difficulties inherent to inertial effects, non-uniform stress/strain distributions and measurements repeatability of the material composite materials behaviour. The use of a servo-hydraulic test machine raises some issues related to the test control variables, notably for interrupted tests [7-9]. Due to the stress-wave propagation, the strain and the stress are non-uniform and hence the strain-rate cannot be spatially constant into the tested specimen. To reduce this difficulty, numerical computations have led to an optimal design of the specimen geometry and the experimental damping system in terms of thickness and material. These simulations were achieved using ABAQUS finite element code [10] and are intended to model the stress wave propagation occurring for a high-speed tensile test. The developed experimental methodology is applied on a Sheet Moulding Compound (SMC-R26).

2. EXPERIMENTAL METHODOLOGY: PROCEDURE AND TESTING DEVICES

2.1 Material description

The tested composite material is a Sheet Moulding Compound noted SMC-R26. It consists of an unsaturated polyester resin reinforced by glass fibres and weakly filled with calcium carbonate fillers ($CaCO_3$). Glass fibres have a weight content of 26 % and are assembled in bundles in such a way that each one contains approximately 200 fibres. These packets of fibres are randomly oriented in the material compression plane and have a constant length (L= 25 mm) with a fibre diameter of 15 µm. The random distribution of reinforcement confers to the material a microscopic heterogeneous aspect and an overall transverse isotropic mechanical behaviour. The SMC-R26 tested plates were prepared of thickness 2.7 mm and were cured at 140 °C with an applied pressure averaging between 7 and 8 MPa for 2 minutes [9]. High-speed tensile tests have been conducted upon a servo-hydraulic test machine. As specified by the manufacturer (Schenck), the test machine can reach a crosshead speed range from 10^{-3} m/s (quasi-static) to 20 m/s. Moreover, the test force level is measured by a piezo-electric crystal load cell of a 50 kN capacity. Strain rates have been estimated exclusively on the basis of strain gauge responses. Tensile tests were carried out at different strain rates according to two ways.

2.2. High-speed tensile tests until rupture

High-strain rate tensile tests were conducted using servo-hydraulic machine at different strain-rates until the composite specimen total failure. The test machine is equipped with a launching system. The composite specimen is positioned between the load cell (upper extremity) and the moving device (lower extremity) as sketched in Fig. 1. Prior to the contact between the sliding bar and the hydraulic jack, the latter is accelerated on a straight displacement of 135 mm in order to achieve the constrained crosshead velocity. Once the contact occurs, the specimen is then subjected to a tension at a constant load-rate. The damping joint placed between the slide and the hydraulic jack may attenuate partially the wave effects caused by the dynamic shock.

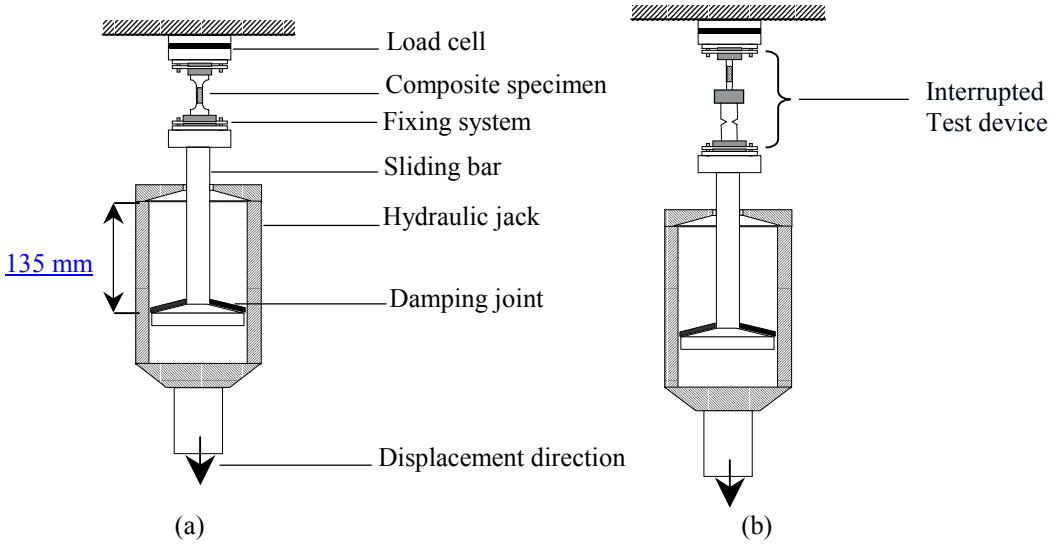

Fig. 1. Schema of the device used for high-speed tensile experiments until specimen rupture (a) and for interrupted high-speed tensile experiment (b) using servo-hydraulic machine.

2.3. Interrupted high-speed tensile tests

The originality of this experimental methodology, proposed by Lataillade et al. [7], consists of the capability to interrupt the specimen loading at fixed stress levels. Indeed, due to inertial effects of the launching system, a rapid tensile test cannot be interrupted until the total failure of the specimen. Accordingly, the specimen is loaded simultaneously with a double-notched

fuse sample (Fig. 1-a) characterised by an elastic brittle fracture. The fuse ligament width is assigned to a suitable level load to be reached when interrupting the loading of the specimen. The above brings about then a stress release in the specimen. This procedure is repeated several times onto the same specimen by changing the fuse (width) before each a new re-loading. One can hence reach a load level greater than the previous.

3. OPTIMISATION OF HIGH-SPEED TENSILE EXPERIMENTS

The damping joint inserted between the sliding bar and the tube of the hydraulic jack enables a partial absorption of the generated stress wave. Nevertheless, the damping joint must be able to attenuate the shock wave during the first stage of its elastic compression. It is obvious that the above affects the load rate. Consequently, an optimal design of the damping joint, in terms of constitutive material and thickness, may result in a constant strain-rate into the tested specimen. For different crosshead velocities, several geometries and materials of the damping joint have been experimentally tested so that gives rise to homogeneous strain/stress in the central zone of the composite specimen. This optimisation led to choose a damping joint consisting of a low impedance material: rubber nitrile of 1.5 mm thickness. Furthermore, composite specimen geometry has been optimised as a result of numerical computations using ABAQUS finite element code. The criterion used for the optimisation consists in reaching a stabilised strain distribution within the specimen gauge section at the beginning of the loading stage. The optimisation procedure relies upon coupling FE numerical results and experimental data. It falls into four stages

i. A tensile test is conducted at a fixed displacement-rate. The displacement induced at specimen extremities is measured. The damping joint, positioned between the sliding and the hydraulic jack, may limit the shock until its total elastic compression corresponding to a rise time noted hereafter (t_r). The latter is averaging between 2.10^{-4} s and 10^{-6} s as a function of the adopted joint thickness and the imposed test velocity. Beyond this time, the composite specimen is therefore subjected to a dynamic loading. The first stage aims then at estimating experimentally the rise time (t_r).

ii. Having estimated the rise time, boundaries conditions are applied on the specimen extremities in terms of imposed velocity, to compute numerically the dynamic response of the specimen.

iii. On the basis of the FE simulations and assuming that the specimen behaves as an elastic solid, a recursive optimisation procedure results in the determination of optimal geometric parameters: L_1, L_2, L_3 and R. These parameters are those of a dumbbell-shaped specimen and are optimised in such a way of reducing the stress wave effects in the overall response and generating homogeneous stress/strain field (Fig. 2).

iv. Finally, high-speed tensile tests are achieved on SMC-R26 composite specimen to validate its optimised geometry. The optimised specimen dimensions are summarised in Table 1.

Table 1. Specimen dimensions optimised for SMC-R26 composite material.

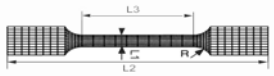	L_1 (mm)	L_2 (mm)	L_3 (mm)	R (mm)
SMC-R26	6	80	30	7

For interrupted high-speed tensile tests, the optimisation procedure is illustrated in the following sections. First, it aims at optimising the fuse and therefore the system consisting of the fuse sample in series with the composite specimen.

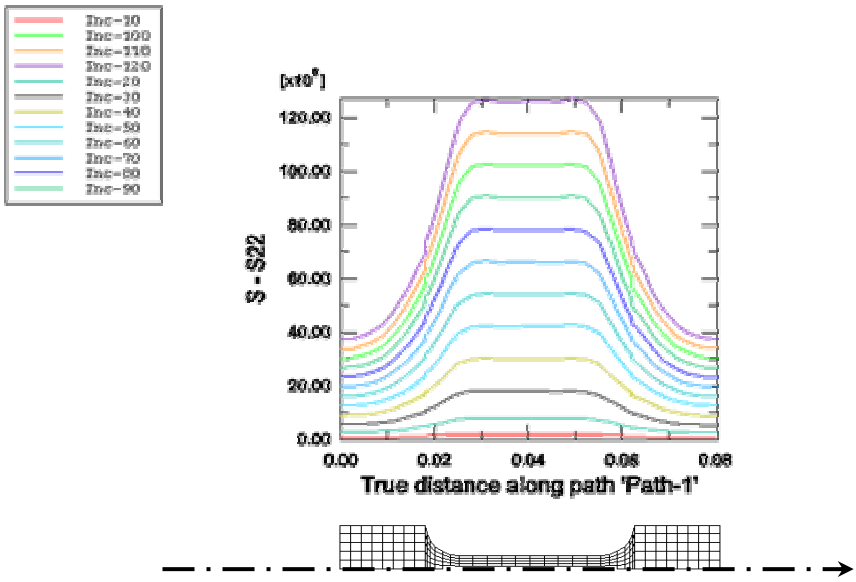

Fig. 2. Spatio-temporal profile of the longitudinal stress (σ_{22}) calculated along the central line of the SMC specimen. Loading conditions: Imposed velocity V=1 m/s giving rise to a strain-rate $\dot{\varepsilon}=20.s^{-1}$

3.1 Optimisation and validation of the fuse geometry

For interrupted high-speed tensile tests, the load level reached prior to an elastic release is assigned to the fuse ligament width. Hence, a preliminary experimental analysis intends to characterise the evolution of the failure load as a function of the ligament width (W). As abovementioned, the fuse must fail as a brittle material and exhibits a linear elastic mechanical response, which should be relatively insensitive to the strain-rate. Several rapid tensile tests were conducted and have allowed retaining a double notched fuse that consisting of polymethylmethacrylate (PMMA). On the basis of the expected load levels, the fuse samples are double notched bars of thickness 4 mm, 80 mm length and 20 mm total width (Fig. 3).

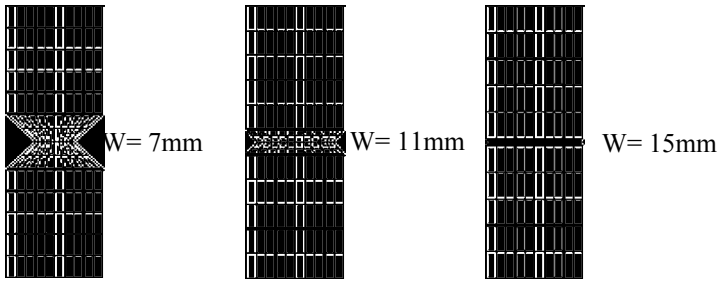

Fig. 3. PMMA double notched fuse geometry with different ligament widths.

Table 2. Correlation between maximal load levels and the ligament width of PMMA fuse. These load levels are estimated for tensile tests performed at 1m/s crosshead displacement rate.

Ligament width (mm)	7	10.5	12	13.5	14.5	15	15.5	16
Maximal load (N)	822	1059	1089	1314	1511	1635	1721	1842

These high-velocity tensile tests have contributed to establish experimentally the relationship between the interrupting load level and the fuse ligament width as illustrated in Table 2.

Using ABAQUS code, numerical simulations were carried out to assess the stress wave propagation involved into the fuse sample during high-velocity tensile tests. Boundary conditions applied for these numerical computations are those defined by experimental

conditions and results. These are applied in terms of rise time ($t_r=10^{-4}$s) and maximal velocity (V_{max}=1m/s). The PMMA fuse is clamped at an extremity and subjected to a constrained displacement-rate. In what follows, numerical results for a velocity (V_{max}=1 m/s) are presented for the fuse specimen with a ligament width W=7 mm. Note that for the others ligament widths, numerical simulations provide similar results. Considering the different time increments, one notices that the front of longitudinal stress wave remains steady close to the fuse notch (Fig. 4). For the whole time steps, FE analysis shows that the stress front is not shifted along the fuse longitudinal line. In addition, the stress distributions, produced during the dynamic event, are numerically estimated along the fuse line as well as along the ligament width. As reported by Fig. 4, these stress distributions exhibit a homothetic increase as a function of time increments. On the basis of these results, one can claim that, in terms of dispersion and perturbation, adopting these experimental conditions may minimize stress wave effects.

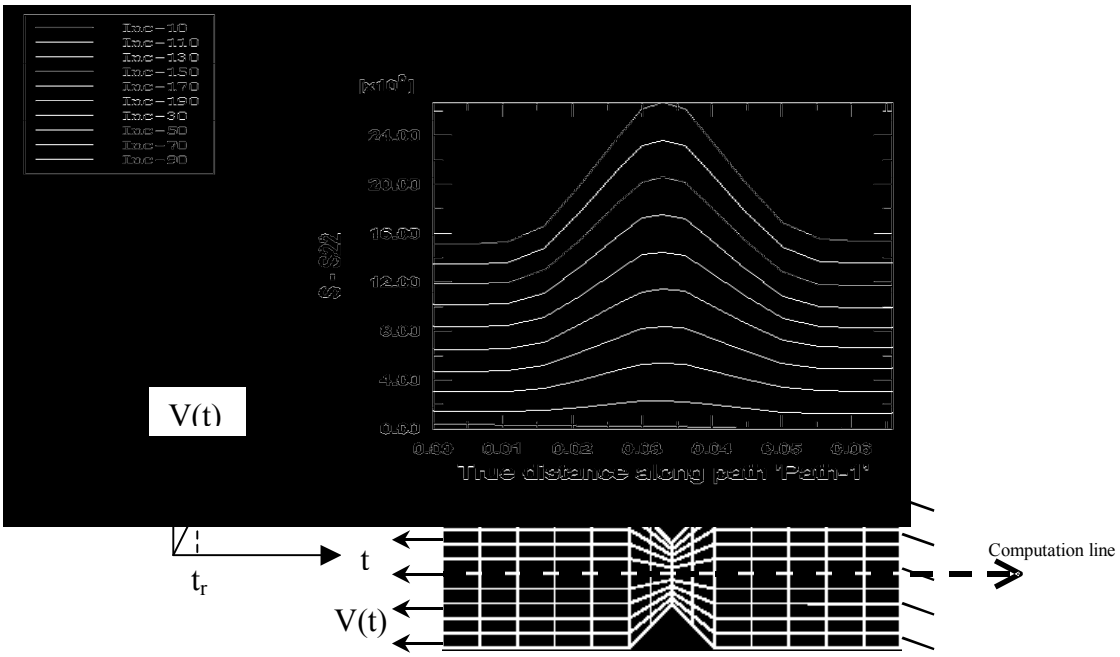

Fig. 4. Numerical predictions of the stress distributions along the fuse line (σ_{22}) estimated for different calculation steps (W=7 mm). SMC-R26

3.2 Optimisation and validation of the system: fuse in series with the composite specimen

The optimisation of the whole system was conducted according to the same stages described in section 3. In what follows the composite specimen is perfectly clamped at the upper extremity and is in series with the PMMA fuse. The latter is fixed to the sliding bar (lower extremity). Numerical computations are performed upon this system subjected to boundary conditions described in section 3-1. These conditions consist of a velocity curve defined by a rise time ($t_r=10^{-4}$s) and maximal velocity (V_{max}=1m/s). SMC composite test specimens are rectangular section tabbed ends bars and having the dimensions of 36x6.5x2.7mm^3. Tabs with tapered ends are bonded on each side of the specimen. These tabs allow a progressive load introduction. They will reduce stress concentration and thus the shock wave stress effects. The adopted specimen geometry was chosen in order to carry out microscopic observations using a scanning electronic microscope (SEM) after each interrupted high-speed tensile test. Fig. 5 shows an example of the stress distribution calculated for different increments load and represented along the central line of the system: fuse-composite specimen. On notices that the fuse exhibits stress profiles and levels identical with those optimised in section 3-1. Furthermore, one observes that stress distribution induced into the composite specimen is

relatively stable in its central zone. For the calculation time increment the longitudinal stress profile increase progressively but remains uniform along the specimen line. Hence, for the adopted experimental conditions one can claim that the dynamic stress wave does not generate parasite effects yielding to a premature damage or failure of the tested specimen. These uniform stress distributions indicate that prior to the damage onset into the tested composite specimen the strain is spatially homogenous and the strain-rate may be constant.

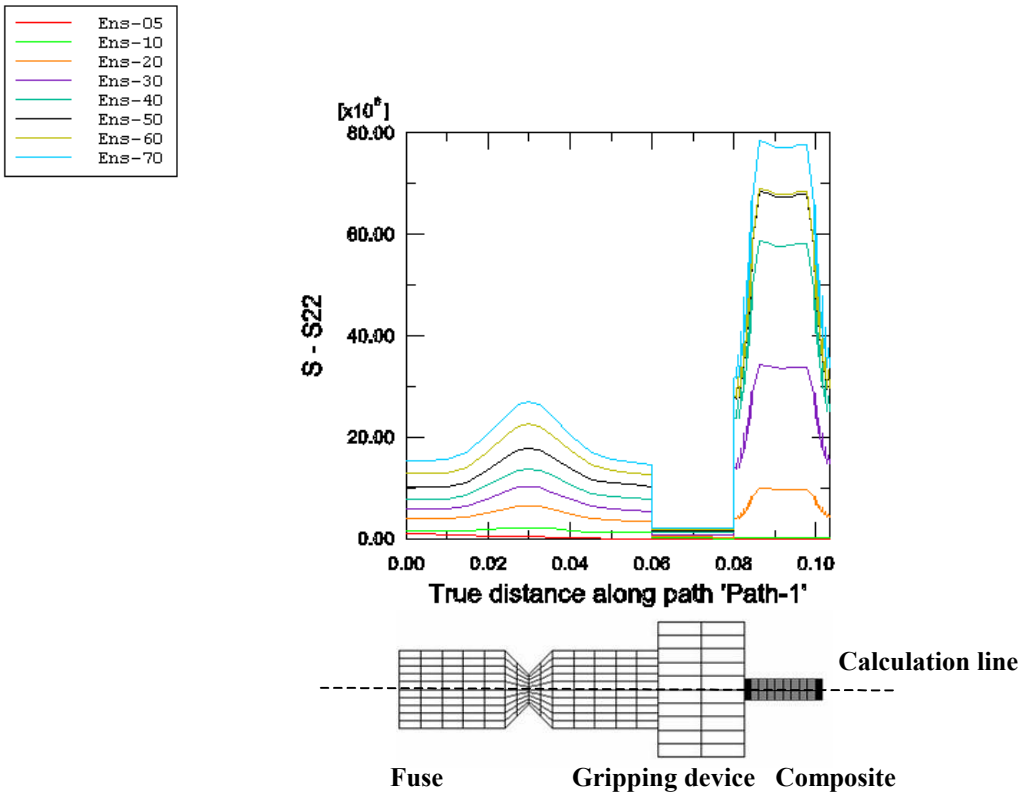

Fig. 5. Longitudinal stress profile calculated along the system fuse-specimen line. SMC-R26

4. EXPERIMENTAL INVESTIGATIONS AND VALIDATION

The developed optimisation methodology is based on experimental tests and coupled to the numerical simulations. It was validated at strain rates up to 200 s^{-1} for Sheet Moulding Compound (SMC-R26)

4.1. Effects of strain-rate on the overall tensile response

The application of the optimised methodology has contributed to investigate the sensitivity of the mechanical characteristics to the strain-rate, in terms of the linear, non-linear behaviour and ultimate properties. These high-speed tensile tests were conducted for the studied material at different strain-rates until the specimen total failure. Note that strain rates have been determined directly on the basis of strain gauges temporal responses.

As shown in Fig. 6, stress-strain (σ–ε) tensile curves plotted for several strain rates show noticeably that the overall behaviour is load-rate dependent. Indeed, under rapid traction SMC-R composites exhibit typically a non-linear response. The beginning of the non-linearity is noticed around 30% of the maximum loading and corresponds to the first stages of the damage growth generated by the matrix micro-cracks leading to interface decohesions. An inflection point, commonly called knee-point, characterizes the latter. Tensile tests were achieved at crosshead velocities from quasi-static to 9 m/s corresponding to strain rates from 10^{-3} to 150 s^{-1}. Fig. 6 shows that initial slopes of the stress-strain curves, estimated for a strain less than 0.3 %, are roughly identical for the different tested strain rates. Therefore, the above

implies that the elastic modulus remain insensitive to the load rate for the tested velocity range. It has a rough average value of 13 GPa. However, the microstructure variability of this class of materials [9, 12-14] can bring about a slight discrepancy notably for dynamic loadings.

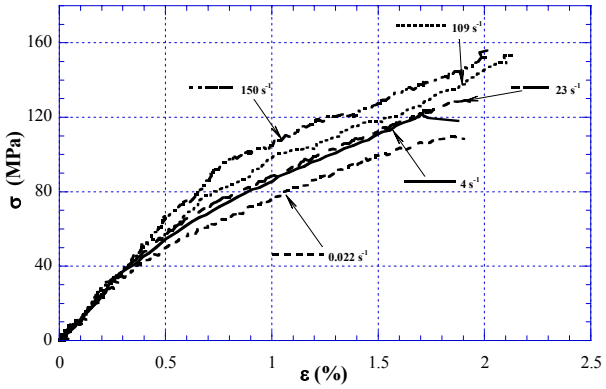

Fig. 6. Experimental strain-stress tensile curves for SMC-R26 composites obtained for testes carried out at strain rate: 0.022, 4, 23, 109 and 150 s^{-1}

Additionally, Fig. 6 indicates that the non-linear stage of the overall response rises moderately as the strain rate increases. Furthermore, a mechanical behaviour accommodation is noticed for the high strain rates. The above arises through an increase of the ultimate strain and stress. Indeed, in terms of stress and strain, ultimate properties and the damage threshold increase significantly for high strain rate. As illustrated in Fig. 7, one can see that the strain rate effect is more noticeable and marked on the ultimate stress than the strain.

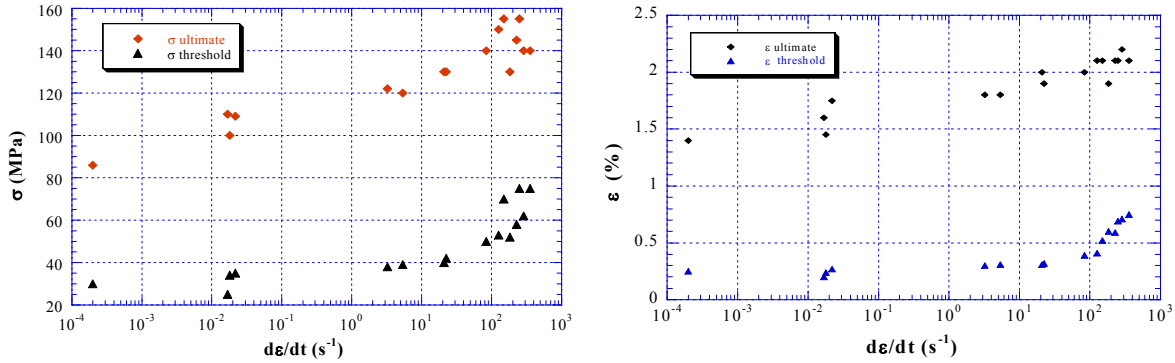

Fig. 7. Effects of strain-rate on the damage threshold and ultimate properties in terms of strain and stress. SMC-R26.

These experimental findings are consistent with those obtained in other works [1-2]. These authors have pointed out that tensile strength increases with strain rate. In addition, one notes a shift of the damage by increasing the strain rate. Actually, when varying the stain rate from the quasi-static to 250 s^{-1}, the stress damage threshold is delayed from 30 MPa to 80 MPa (Fig. 14). While, the strain damage onset increases from 0.25 % to 0.77 %.

4.2. Effects of strain-rate on the damage onset and kinetic

Interrupted high-speed tensile tests have widely contributed to evaluate the rate dependence of the damage in terms of initiation and kinetic of the experimented composite. Damage analysis was conducted according to two ways. The first intends to estimate the macroscopic Young's modulus reduction (D_{macro}) whereas the second aims at quantifying the damage accumulation (d_{micro}) at the microscopic material scale. Several works focusing on damage in polymer reinforced fibre composites have been conducted using different

experimental techniques such as acoustic emission [11], micrographs, C-Scan. They pointed out that composite materials fail through a sequence of damage mechanisms, namely: matrix microcracking, fibre-matrix debonding, interfacial decohesion and fibre breakage. The three first processes often instigate a progressive material degradation involving therefore a high-energy dissipation, whereas the last mechanism precedes the material collapse. Macroscopic damage can be quantified by the tensile modulus reduction using the well-known damage mechanics [12]. The damage scalar parameter is thus expressed such as:

$$D_{\text{macro}} = 1 - \frac{E^D}{E^0}$$

E^0 and E^D, are respectively the Young's modulus of virgin and damaged material. (E^0) is determined by the initial slope of the stress-strain curve. The current modulus (E^D) is estimated by the slope of the reloading curve after to each tensile test interruption at a predefined load level.

Additionally, the local damage estimation aims at establishing a relationship between the micro-defects density, generated by the interface decohesions, and the macroscopic strain/stress applied level. After each interrupted tensile test, damage accumulation is investigated by means of SEM micrographs performed upon a representative element volume (REV). Specimen cartography is achieved using image-analysis. These contribute to characterizing the bundles degradation, in terms of matrix micro-cracks and fibre-matrix debonding. This investigation results in a quantitative damage evaluation by estimating defects effects. For that, one defines first a microstructural parameter describing the debonded fibres content (f_d). The microscopic damage state is then represented at the local scale as:

$$d_{\text{micro}} = \frac{f_d}{f_v}$$

f_d is the volume fraction of debonded fibres and f_V is the fibre volume content in the (REV).

Interrupted high-speed tensile tests have been achieved on SMC-R26 composite for the following strain rates: 0.0002, 3, 8 and 20 s^{-1}. These correspond respectively to crosshead velocities of 2.10^{-4}, 0.2, 0.5 and 1 m/s. SMC-R26 specimens are rectangular section tabbed ends bars. Dimensions are resulting from the optimisation procedure: 36x6.5x2.7mm^3.

As detailed in section 2-2, the specimen is loaded in series with a brittle fuse (PMMA). By changing the fuse width, one can interrupt the high-speed test at a fixed load level. This procedure is repeated several times on the same specimen increasing the fuse width before each new re-loading. For each "unloading/re-loading" loop, the evolution of the damage parameter (D_{macro}) is experimentally estimated.

As reported in Fig. 8, the evolution of the macroscopic damage parameter is plotted against the strain level for three tested strain rates.

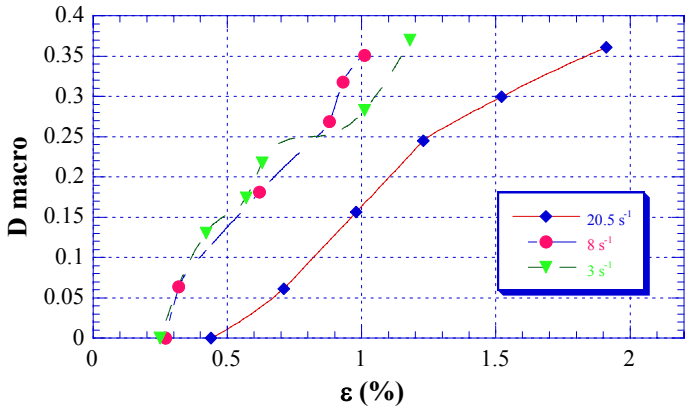

Fig. 8. Longitudinal Young's modulus reduction evolution vs. applied strain and plotted for different strain-rate. SMC-R26.

Experimental findings from interrupted tensile tests confirm that increasing the strain rate leads to a delayed macroscopic damage initiation. Indeed, for a a strain rate of $3s^{-1}$, macroscopic degradation begins at a strain level of 0.25% when for a strain rate of $20s^{-1}$, the first stiffness reduction appears at a strain in the order of 0.43%. Hence, it easily follows that the damage evolution is relatively reduced as the crosshead rate increases from quasi-static to intermediate. Thus, one can claim that the stiffness reduction is rate dependent.
Besides the stiffness reduction analysis, a microscopic investigation was conducted to relate the micro-defects density and the macroscopic strain/stress applied level. This microscopic analysis is achieved by means of SEM micrographs performed upon a representative element volume (REV). It is worthy to note that the investigation zone is considered as representative of the material microstructure. In addition, microscopic observations have established that this zone is statistically representative for the damage accumulation. Nevertheless, it must be emphasized that the micro-defects coalescence is increased for reinforcements having an orthogonal orientation with the maximum stress direction. However, it remains confined and limited for the fibres less oriented (Fig. 9).

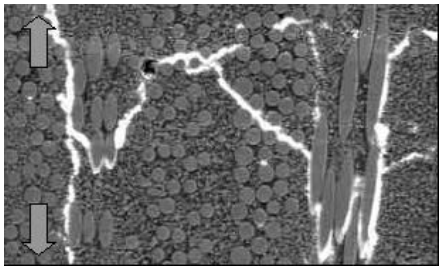

Fig. 9. Matrix micro-cracks coalescence leading to interfacial decohesion. SMC-R26 ($\dot{\varepsilon}$ =20 s^{-1})

Fig. 10 illustrates the accumulation of micro-defects, generated by the interface decohesions, as a function of the macroscopic strain level. One observes that at the local scale the damage growth is shifted in term of strain and exhibits a lessened kinetic due to the strain rate effect. Both aspects are related to the viscous effect generated by the delay of the dissipation occurring at interfacial zones. Consequently, one notices a lag in the macroscopic damage initiation coupled to a slight decreasing in term of its evolution.

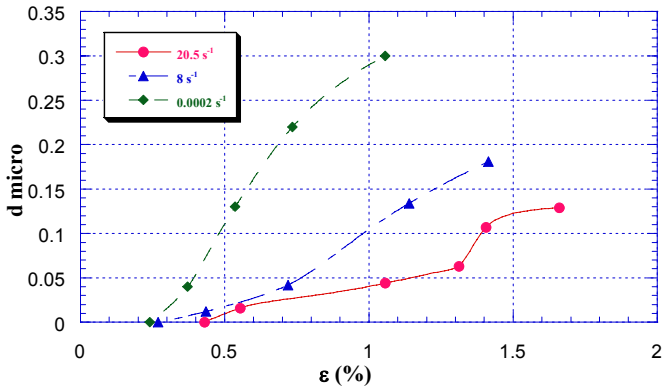

Fig. 10. Evolution of damage parameter (d_{micro}) vs. applied strain and plotted for different strain-rate. SMC-R26.

5. CONCLUSION

The present work has proved that servo-hydraulic testing machine may be suitable to examine strain-rate effects on overall composite behaviour for a moderate rates up to $200s^{-1}$. Nevertheless, success with the high strain rate testing of polymer composites requires an experimental methodology able to isolate inertial disturbances attributed to the test system. To this end, an experimental methodology has been developed and optimised. It aims at minimizing the amplitude of measurements perturbation for giving rise to homogeneous stress/strain fields within the tested specimen. Experimental findings, obtained from monotonic and interrupted tensile tests performed at different strain rate, were input in numerical computations using ABAQUS FE code for optimising iteratively the experimental conditions. The analysis of the stress wave propagation occurring for a high-speed tensile test has resulted in an optimal design of the specimen geometry and the experimental damping system: thickness and material characteristics. On one hand, the optimisation has contributed to generate uniform strain and stress fields yielding hence to a strain-rate spatially constant into the tested specimen. One the other hand, it has enabled to set up the interrupted high-speed tensile tests. These have provided the monitoring of the stiffness reduction evolution and the damage accumulation by interrupting the test at predefined load levels.
The developed experimental methodology based on dynamic tensile tests has contributed to emphasize the strain rate effects on overall behaviour of SMC-R26. As the strain rate increased, noticeable effects consist of a delayed damage onset followed by a slightly reduced damage accumulation. It was established that the strain rate brings about a viscous nature of damage evolution leading hence to the notion of the visco-damaged behaviour. Due to the time-dependant damaged-behaviour, the interface strengths are increased, which explains readily the accommodation exhibited at the macroscopic scale. As the strain rate increases, the damage viscosity reduces then the material degradation and the damage kinetic.

6. References

1. **Okoli OI, Smith GF**. High strain rate characterization of a glass/epoxy composite. J Compos Technolo Res, JCTRER 2000;22(1): 3-11.
2. **Okoli OI.** The effects of strain rate and failure modes on the failure energy of fibre reinforced composites. Composite Structure 2001; 54: 299-303;
3. **Harding J, Welsh LM**. A tensile testing technique for fibre-reinforced composites at impact rates of strain. J Mater Sci, 1983;18:1810-26.
4. **Rodney J.** Clifton. Response of materials under dynamic loading. International Journal of Solids and Structures 37 (2000) 105-113
5. **Dear JP, Brown SA**. Impact damage in reinforced polymeric materials *Composites. Part A: Applied Science & Manufacturing,* 34(2003) 411-420.
6. **H. M. Hsiaoa and I. M. Daniel**, Strain rate behavior of composite materials. *Composites Part B* 29B (1998) 521–533
7. **Lataillade J-L., Delaet M., Collombet F., Wolff C**. Effects of the intralaminar shear loading rate on the damage of multi-ply composites. Int. J. Impact Engng 1996; 18-6: 679-699.
8. **Pardo S., Baptiste D., Décobert F., Fitoussi J., Joannic R**. Tensile dynamic behaviour of a quasi-unidirectional E-glass/polyester composite. Composites Science and Technology 2002; 62(4): 579-584.
9. **Jendli Z., Meraghni F.**, **Fitoussi J., Baptiste D.** Micromechanical analysis of strain rate effect on damage evolution in Sheet Molding Compound composites. (in-press) *Composites. Part A: Applied Science & Manufacturing, 2004*
10. **HKS Inc**, ABAQUS Theory and Users Manuals V. 6.2.1, 2001.
11. **Meraghni F., Desrumaux F., Benzeggagh M. L.** Implementation of a constitutive micromechanical model for damage analysis in glass mat reinforced composites structures. Composites Science and Technology 2002; 62: 2087-2097.
12. **Krajicnovic D.** Selection of damage parameter – Art or science? Mechanics of Materials 1998; 28: 165-179.